

Article

A Bayesian Analysis of Plant DNA Length Distribution via κ -Statistics

Maxsuel M. F. de Lima ¹, Dory H. A. L. Anselmo ^{1,2,*}, Raimundo Silva ^{1,2}, Glauber H. S. Nunes ³, Umberto L. Fulco ⁴, Manoel S. Vasconcelos ² and Vamberto D. Mello ¹

¹ Departamento de Física, Universidade do Estado do Rio Grande do Norte, Natal 59072-970, RN, Brazil

² Departamento de Física, Universidade Federal do Rio Grande do Norte, Natal 59072-970, RN, Brazil

³ Departamento de Ciências Vegetais, Universidade Federal Rural do Semi-Árido, Mossoró 59625-900, RN, Brazil

⁴ Departamento de Biofísica e Farmacologia, Universidade Federal do Rio Grande do Norte, Natal 59072-970, RN, Brazil

* Correspondence: doryh@fisica.ufrn.br

Abstract: We report an analysis of the distribution of lengths of plant DNA (exons). Three species of *Cucurbitaceae* were investigated. In our study, we used two distinct κ distribution functions, namely, κ -Maxwellian and double- κ , to fit the length distributions. To determine which distribution has the best fitting, we made a Bayesian analysis of the models. Furthermore, we filtered the data, removing outliers, through a box plot analysis. Our findings show that the sum of κ -exponentials is the most appropriate to adjust the distribution curves and that the values of the κ parameter do not undergo considerable changes after filtering. Furthermore, for the analyzed species, there is a tendency for the κ parameter to lay within the interval (0.27; 0.43).

Keywords: DNA; *cucurbitaceae*; non-additive statistics



Citation: de Lima, M.M.F.; Anselmo, D.H.A.L.; Silva, R.; Nunes, G.H.S.; Fulco, U.L.; Vasconcelos, M.S.; Mello, V.D. A Bayesian Analysis of Plant DNA Length Distribution via κ -Statistics. *Entropy* **2022**, *24*, 1225.

<https://doi.org/10.3390/e24091225>

Academic Editors: Antonio M. Scarfone, Dionissios T. Hristopulos and Sergio Luiz E. F. da Silva

Received: 15 August 2022

Accepted: 31 August 2022

Published: 1 September 2022

Publisher's Note: MDPI stays neutral with regard to jurisdictional claims in published maps and institutional affiliations.



Copyright: © 2022 by the authors. Licensee MDPI, Basel, Switzerland. This article is an open access article distributed under the terms and conditions of the Creative Commons Attribution (CC BY) license (<https://creativecommons.org/licenses/by/4.0/>).

1. Introduction

There are 15 tribes in the family Cucurbitaceae [1]. The tribe Cucurbitae, which has an almost completely American distribution, consists of 11 genera, including the genus *Cucurbita*. The genus *Cucurbita* (Cucurbitaceae) has five major domesticated species: *Cucurbita moschata*, *Cucurbita pepo*, *Cucurbita maxima*, *Cucurbita argyrosperma*, and *Cucurbita ficifolia* [2,3].

The first three species cited are the most economically important as a popular food resource [4]. The fruits of the species are incredibly diverse, differing greatly in shape, surface topography, color, size, and color pattern [5]. Among them, *C. pepo* is the genus' most phenotypically variable species and has eight cultivar groups with edible fruits (groups) [6]. The second most diversified species in the genus is thought to be *C. moschata* [7].

All *Cucurbita* species have 20 pairs of chromosomes ($2n = 2x = 40$), making them all diploid. The theory that Cucurbiteae underwent one whole-genome duplication as a result of their high chromosome number has gained traction [8,9]. The tribe Cucurbiteae plant species, including the zucchini (*C. pepo*), pumpkin (*C. moschata* and *C. maxima*), and silver-seed gourd (*C. argyrosperma*), all suffered whole-genome duplication events, according to a number of studies [9–11].

There are few estimates of genome size in the genus *Cucurbita*. However, studies have shown relatively small genome sizes. The genome sizes of *C. maxima* and *C. moschata* were estimated to be 271.40 and 269.90 Mb, respectively, [9], while the genome size in *C. pepo* was estimated to be 263.0 Mb [10]. Concerning the number of genes, the estimated values for *C. maxima*, *C. moschata*, and *C. pepo* were 32,076; 32,205 [9]; and 27,868 genes [10], respectively.

On the other hand, numerous models based on statistical physics consistently attempt to represent statistical features, such as long-range and short-range correlations, in light of

the large DNA sequence data. Some approaches used statistical tools in connection with random-walk simulations [12–14], wavelet transforms [15,16], 1D Ising models [17] (see e.g., [18] and references therein), and Tsallis' statistics together with Machine Learning [19]. Many live creatures' coding and non-coding sequence length distributions have been studied by some models in relation to long- and short-range correlations [20–23]. Non-additive entropy-based statistical physics methods have recently been actively advocated for use in complex system research [24,25]. In this case, the Kaniadakis entropy yields a power-law distribution rather than an exponential one and depends on a free parameter (the κ parameter) [26–28]. The κ -statistics arose as a useful statistical tool for many systems (see [29] and references therein). For problems associated with human DNA, see e.g., [30,31].

Additionally, the Bayesian inference has been effectively applied as a useful tool to investigate a number of issues in physics [32] and biophysics [33]. Which DNA models should be valid from the perspective of Bayesian inference is an intriguing subject. Additionally, the challenge in the context of this work would be to investigate an expansion of a model from Ref. [31], but this time in the context of other living structures, such as vegetables.

More recently in [34], statistical models of the Tsallis type provided the distribution of nucleotide chain lengths, successfully capturing the statistical correlations between the parts of the plant (for both coding and non-coding) DNA strands for two species of the Cucurbitaceae family. We expand the paradigm proposed in [31] in the context of vegetables in this article. We especially evaluate the distribution of nucleotide chain lengths measured in base pairs for *Cucurbita maxima*, *Cucurbita moschata*, and *Cucurbita pepo* utilizing κ -deformed statistics in light of the social and economic significance of cucurbits. The most practical model is then chosen using a Bayesian statistical analysis based on the κ -distributions. To the best of our knowledge, this is the first time the size distribution of plant DNA has been realized using a κ -statistical analysis.

2. Materials and Methods

We use the κ -statistics, developed by Kaniadakis [26–28], to analyze the correlations between the DNA length distributions of some species of the *Cucurbitaceae* family. There are some works in this direction using the Tsallis q -statistics [34–36]. The κ -entropy and power-law distribution functions naturally arise from the kinetic foundations of κ -statistics. Formally, the κ -framework is based on the κ -exponential and κ -logarithm functions (see Ref. [26]), defined as

$$\exp_{\kappa}(x) = \left[\sqrt{1 + \kappa^2 x^2} + \kappa x \right]^{\frac{1}{\kappa}} \quad (1)$$

$$\ln_{\kappa}(x) = \frac{x^{\kappa} - x^{-\kappa}}{2\kappa}. \quad (2)$$

The parameter κ is restricted to values belonging to the range $|\kappa| < 1$; for $\kappa = 0$, these expressions reduce to the usual exponential and logarithmic functions. From the optimization of entropy S_{κ} (see Ref. [37]), we can obtain the probability distributions ($P_{\kappa,1}(l)$) associated with the quantities of base pairs (*bp*) for each of the chromosomes of *Cucurbita maxima*, *Cucurbita moschata*, and *Cucurbita pepo*. Mathematically, the Kaniadakis entropy S_{κ} is given by

$$S_{\kappa}(l) = -\frac{1}{2\kappa} \int_{\kappa} \left[\frac{1}{1+\kappa} P_{\kappa}(l)^{(1+\kappa)} - \frac{1}{1-\kappa} P_{\kappa}(l)^{(1-\kappa)} \right] dl. \quad (3)$$

The optimization process is well described in Refs. [26,37–41] and gives us $P_{\kappa,1}(l)$

$$P_{\kappa,1}(l) = (1 - \kappa^2) \beta \exp_{\kappa}[-\beta l]. \quad (4)$$

Rewriting (4) with the explicit form of $\exp_\kappa(-\beta l)$ given by (1), and using constraints as in Ref. [41], we get

$$P_{\kappa,1}(l) = \frac{(1-\kappa^2)}{L_\kappa} \left[\sqrt{1 + \kappa^2 \left(-\frac{l}{L_\kappa} \right)^2} + \kappa \left(-\frac{l}{L_\kappa} \right) \right]^{\frac{1}{\kappa}}. \quad (5)$$

Here, L_κ is an adjustable parameter that is related to the mean value of the length distribution, κ is the model's free parameter which measures the interaction between the nucleotides in the sample, and l is the chain of nucleotides' length, expressed in number of base pairs.

We employ the cumulative probability distribution because the probabilities for lengthy lengths l of the nucleotide chain are subject to significant fluctuations.

We employ the cumulative probability distribution because the probabilities for lengthy lengths l of the nucleotide chain are subject to significant fluctuations, (5) can be found by solving $\Phi(l) = p(l' < l) = \int_0^l p(l') dl'$, which provides

$$\Phi_{\kappa,1}(l) = 1 - \frac{1}{2} [G_\kappa^+(l) + G_\kappa^-(l)], \quad (6)$$

where

$$G_\kappa^\pm(l) = (1 \pm \kappa) \exp^{1 \mp \kappa} \left(-\frac{l}{L_\kappa} \right). \quad (7)$$

Here, $\Phi(l)$ denotes the probability of finding the sizes of the bases between 0 and l . In Ref. [34], it was proposed a comparison between the q -exponential and a sum of q -exponentials to explain the DNA length distribution of two species of cucurbits, *Cucumis melo* and *Cucumis sativus*. Based on this work, we propose an analysis of the same type but using the κ -statistics. We assume that the sum of Kaniadakis-type generalized probabilities (already normalized) is given by

$$P_{\kappa,2}(l) = (1 - \kappa^2) \left[\frac{\gamma_1 \gamma_2}{\gamma_1 + \gamma_2} \right] [\exp_\kappa(-\gamma_1 l) + \exp_\kappa(-\gamma_2 l)], \quad (8)$$

where κ , γ_1 , and γ_2 are adjustable parameters and l is the length of the nucleotides, respectively. By employing the identical steps as those leading to (6), the cumulative probability distribution is found to be

$$\Phi_{\kappa,2}(l) = 1 - \left[\frac{1}{\gamma_1} F_{1,\kappa}(l) + \frac{1}{\gamma_2} F_{2,\kappa}(l) \right], \quad (9)$$

where

$$F_{j,\kappa}(l) = \frac{\gamma_1 \gamma_2}{\gamma_1 + \gamma_2} \left[\frac{\exp_\kappa^{1-\kappa}(-\gamma_j l)}{1 - \kappa} + \frac{\exp_\kappa^{1+\kappa}(-\gamma_j l)}{1 + \kappa} \right], \quad j = 1, 2. \quad (10)$$

Initial analyses indicate that, as occurred for the Tsallis' q -statistics [34], the κ -exponential sum model best fits the DNA length distributions of the species studied here. Therefore, we chose to make a comparison between the sum of κ -exponentials (9) and the κ -Maxwellian model (11) below, proposed in [31] to explain the length distribution of human DNA.

$$\Phi_{\kappa,3}(l) = 1 - \exp_\kappa \left(-\frac{l^2}{\sigma_\kappa^2} \right) \left[\sqrt{1 + \kappa^2 \frac{l^4}{\sigma_\kappa^4}} + \kappa^2 \frac{l^2}{\sigma_\kappa^2} \right]. \quad (11)$$

The best model to describe the length distributions of the nucleotides for three species of the *Cucurbitaceae* family is obtained by comparing, via Bayesian analysis, the distributions $\Phi_{\kappa,2}(l)$ and $\Phi_{\kappa,3}(l)$, which are represented by Equations (9) and (11), respectively.

3. Results

We use the public database of the National Center for Biotechnology Information (NCBI) [42] and the Comparative Genomics (CoGe) [43]. They are databases that give users access to genetic and biological data. In our analysis, we considered only the coding bases (exons). We define a nucleotide sequence's length in terms of the l (bp) base pairs. All graphical and data modeling was written in R, a free statistical software [44].

By plotting the cumulative probability distribution function (CDF) and a box plot for chromosome 02 of one of the species studied here (Figure 1), we can see that some points are very far from the distribution and can be considered outliers. There are various techniques for defining, spotting, and dealing with outliers [45]. In this work, we decided to use the box plot approach. Outliers in this approach are points that are below the region $Q1 - 1.5 \times IQR$ and above $Q3 + 1.5 \times IQR$, where $Q1$, $Q2$, and $Q3$ are first, second, and third quartile, respectively, and IQR is the interquartile region defined as $IQR = Q3 - Q1$. To prevent these points from influencing the behavior of the proposed models, we decided to remove them. The cut was made around 1% of the cumulative distribution, designated by the hatched square in the lower right corner of Figure 1a. A similar approach has been proposed in [46] to analyze the length distribution of human DNA. Table A1 describes the statistical characteristics of some chromosomes of the three species of *Cucurbitaceae* after removing these outliers.

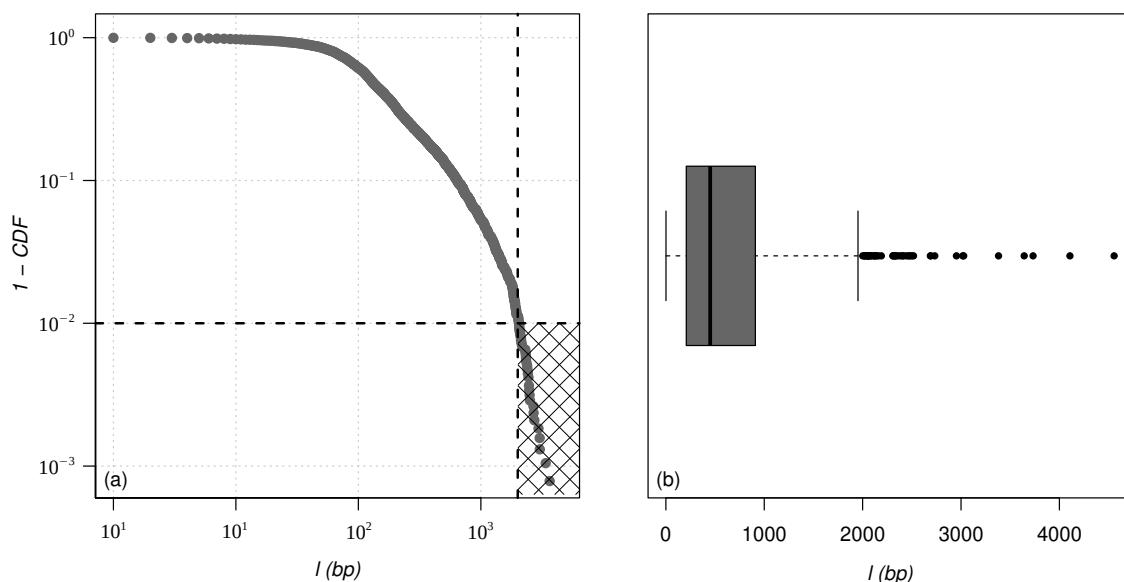


Figure 1. (a) Cumulative probability distribution function (CDF) and (b) box-plot for chromosome 02 of the species *Cucurbita maxima*. A similar analysis was performed for all chromosomes of the three species of *cucurbitaceae* studied in this paper.

We decided to analyze the impact this action had on the value of κ , taking into account the cumulative distribution functions (9) and (11). In Tables A2 and A3, we have the number of nucleotides (N) and the best fit values per κ . The subscripts 0 and f represent the values before and after the outliers are removed, and (RD) represents the relative difference between them. The values of RD are smaller than the errors associated with the values of κ in Tables A4–A6. This work deals with a statistical analysis of the distribution of DNA lengths in plants. Possible biological effects caused by removing nucleotides with large amounts of base pairs were not taken into account.

In Figures 2–4, we show the cumulative distributions, for exons, for some chromosomes of *Cucurbita maxima*, *Cucurbita moschata*, and *Cucurbita pepo*, with the other chromosomes behaving similarly. To get the best fit values for κ , the distribution functions (9) and (11) were fitted to the lengths (l). Tables A4–A6 show all numerical results for the parameters κ , γ_1 and γ_2 for distribution (9) in addition to κ and σ_κ for distribution (11).

Chromosome numbers are displayed in the first column (CHR), and the number of nucleotide chains is displayed in the second column (N) (exons). The correlations between the values of l are measured by the values of κ [26–28,39]. According to [36,47], the coding part of human DNA tends to present short-range correlations. The same behavior for plant DNA can be observed in [34]. This implies κ values close to zero. It is worth remembering that in the limit $\kappa \rightarrow 0$, we return to the well-known Boltzmann–Gibbs–Shannon statistics [26].

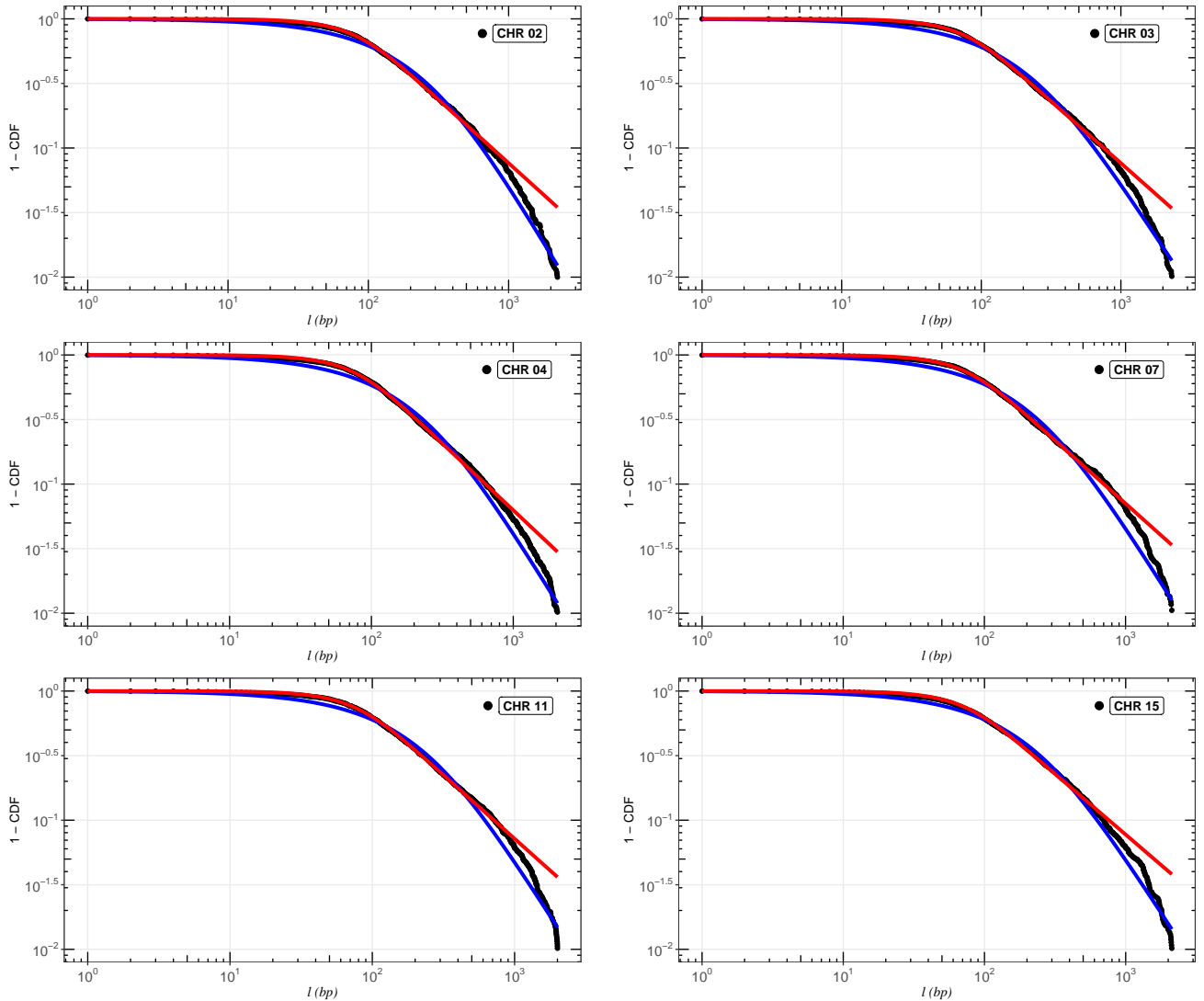


Figure 2. Best fit analysis for the exons of *Cucurbita maxima*. We can observe the adjustments for chromosomes (CHR) 02, 03, 04, 07, 11, and 15. The blue and red curves are, respectively, the distributions (9) and (11). The other chromosomes follow the same pattern.

The models that fit the length distribution $\Phi(l)$ the best are determined via Bayesian statistics. By taking into account the probability distribution of the hypotheses, conditioned on the evidence, Bayesian inference describes the relationship between the model and the data, and enables a rational and effective selection of one or more hypotheses [48]. The Bayes' theorem,

$$P(\Phi|D, M) = \frac{\mathcal{L}(D|\Phi, M) \cdot P(\Phi|M)}{\mathcal{E}(D|M)}, \quad (12)$$

offers us the likelihood that, given the data D , a posterior model Φ will be correct. For this, the probability of the prior model $P(\Phi|M)$ is multiplied by the likelihood function $\mathcal{L}(D|\Phi, M)$ and divided by the Bayesian evidence $\mathcal{E}(D|M)$. Here, we assume the pattern

$\chi^2 = (P(l^{obs}) - P(l^{the}))^2 / \sigma_{obs}^2$ for the likelihood function, where $P(l^{obs})$, $P(l^{the})$ and σ_{obs} are the cumulative probabilities associated with the observed and the theoretical nucleotide lengths, and observed errors, respectively.

The input parameters used in the prior uniform distribution were obtained from the best fit found by the R-code. This approach, which defines the model parameters' potential range and significantly affects the Bayesian evidence, is a crucial phase in the study. This condition ensures that the parameters will fall inside the previously identified optimal adjustment range.

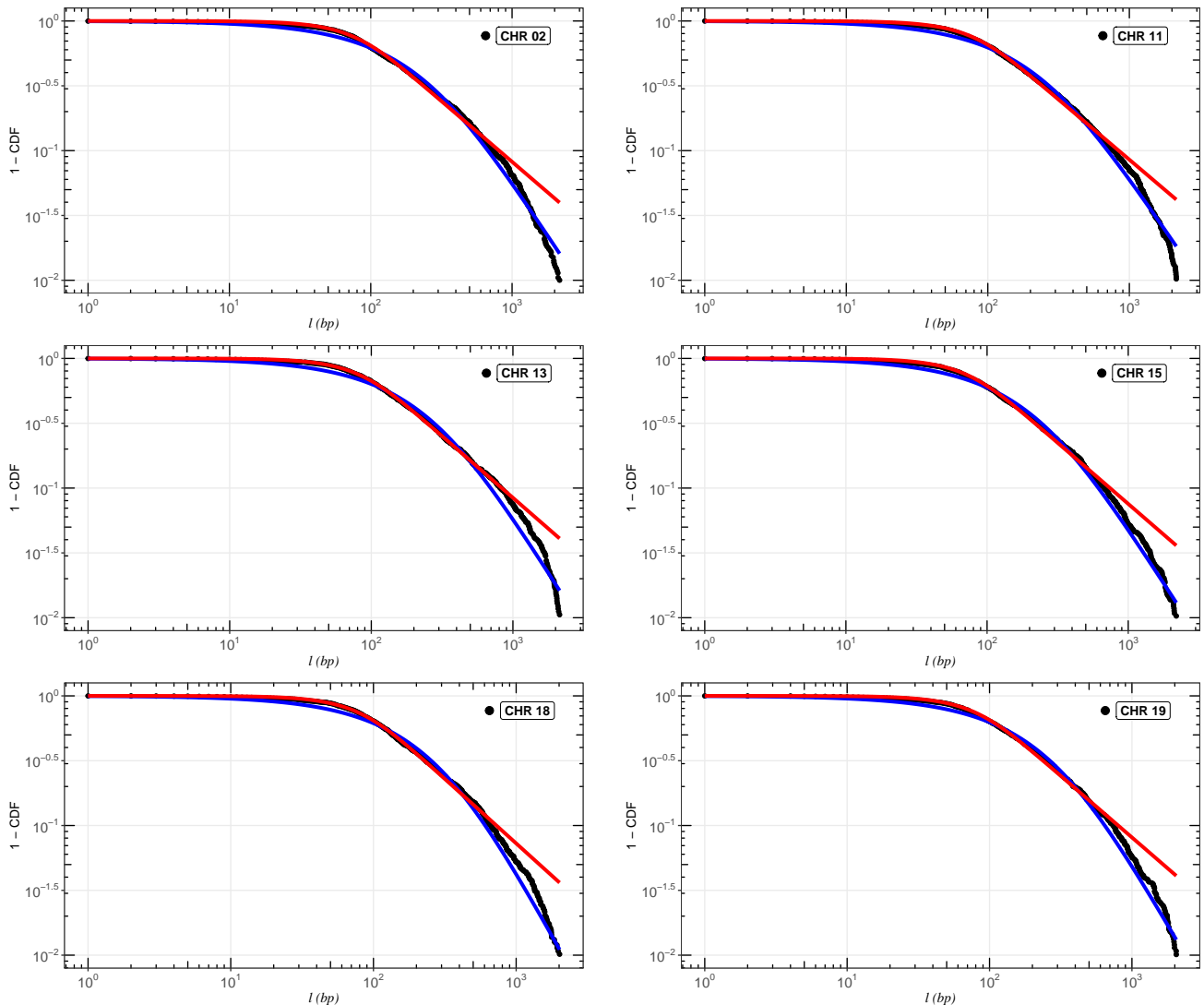


Figure 3. Best fit analysis for the exons of *Cucurbita Moschata*. We can observe the adjustments for chromosomes (CHR) 02, 11, 13, 15, 18, and 19. The blue and red curves are, respectively, the distributions (9) and (11). The other chromosomes follow the same pattern.

In Table A4, we have the parameter ranges for *Cucubita maxima*. Considering all chromosomes (CHR), $\kappa_M \sim U(0.64, 0.69)$, $\sigma_\kappa \sim U(91, 105)$, for cumulative distribution (11), and $\kappa_S \sim U(0.24, 0.39)$, $\gamma_1 \sim U(0.0041, 0.0087)$ and $\gamma_2 \sim U(0.0045, 0.0088)$ for cumulative distribution (9). The process is repeated for the species *Cucubita moschata* in Table A5 and *Cucubita pepo* in Table A6. The MULTINEST algorithm, a Bayesian inference tool that computes the evidence $\mathcal{E}(D|M)$ with an associated error estimate, is thus put into practice for each species and each model. It generates posterior samples from distributions that can contain multiple modes and pronounced degeneracy (curves) in high dimensions. More details can be seen in [49–53].

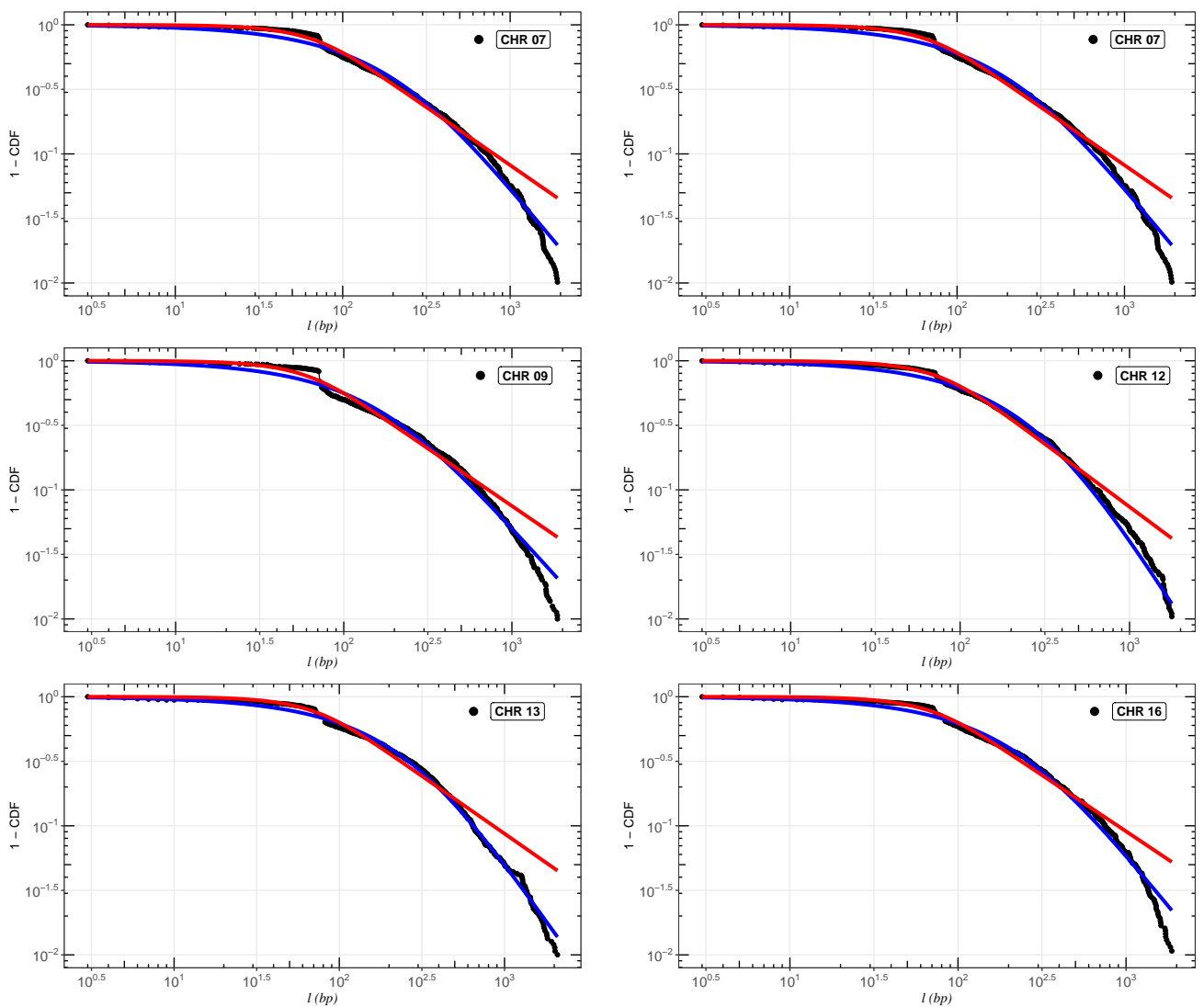


Figure 4. Best fit analysis for the exons of *Cucurbita Pepo*. We can observe the adjustments for chromosomes (CHR) 01, 07, 09, 12, 13, and 16. The blue and red curves are, respectively, the distributions (9) and (11). The other chromosomes follow the same pattern.

In order to compare the models, we make use of the Bayes factor, which is given by

$$B_{ij} = \frac{\mathcal{E}_i}{\mathcal{E}_j}. \quad (13)$$

Here, \mathcal{E}_j is the evidence of the base model, which is used as a reference. In our case, this is the distribution (9), and \mathcal{E}_i is the evidence of the model we want to compare, given by distribution (11). We employ the Bayes factor interpretation provided by Jeffrey's theory [35,54–56] to measure whether a model has favorable evidence in comparison to the base model. Table A7 contains the findings for each chromosome.

The Bayesian analysis is performed from each model's range of definite parameters. Therefore, the better we understand the behavior of the parameters, the more accurate our analysis will be, and we can guarantee that the evidence found will represent the curve with the best fit [48]. In Figures 5–7, we have scatter plots for the parameters of the models (9) (a) and (11) (b). For all chromosomes of all species analyzed here, we found strong correlations between the parameters γ_1 and γ_2 present in the distribution (9). This was expected, as this model appears as a variation of the model (6), as carried out in [34]. These two adjustable constants together (γ_1 and γ_2) have an inverse role to what L_K has in

the distribution (6), and when $\gamma_1 = \gamma_2$, we obtain the model (6) again. This implies that these parameters are related to the κ parameter in the same way, resulting in similar images for scattering but with different ranges. This behavior was repeated for all chromosomes.

The κ_S parameter (that is, the κ value that provides the best fit, when using the sum of κ -exponentials, Equation (9)) in Tables A4–A6, measures the correlation between lengths l , and belongs to the range (0.27(4); 0.37(2)) in the case of *Cucubita maxima*, (0.28(3); 0.40(4)) for *Cucubita moschata*, and (0.32(3); 0.43(3)) for *Cucubita pepo*. It can be seen in Figure 8 that the values of κ , for different species, seem to specify a universal behavior. Therefore, all of these findings lead us to the conclusion that for all the species under study, the model (9) (sum of κ -exponentials) is strongly preferred over the distribution model (11) (κ -Maxwellian).

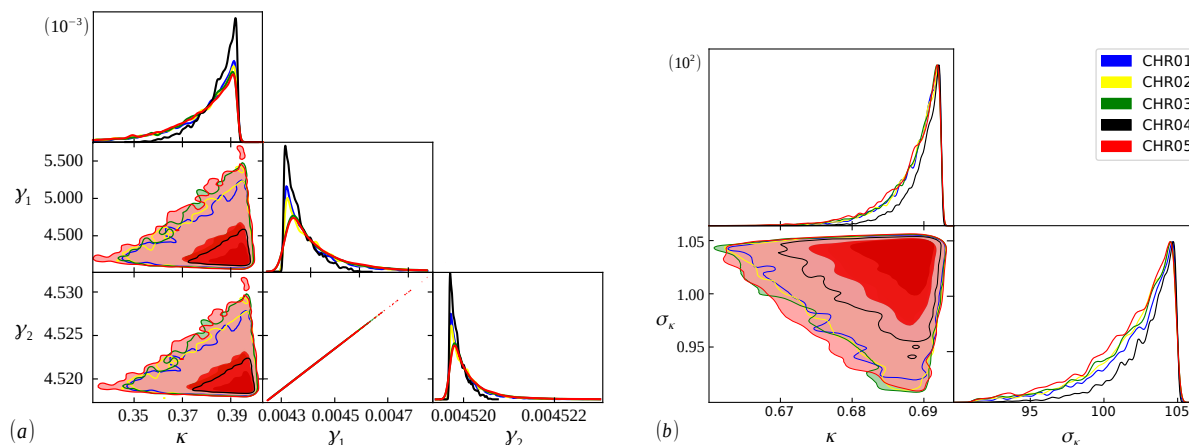


Figure 5. Bayesian analysis for the (9) (a) and (11) (b) distributions, using chromosomes 01, 02, 03, 04, and 05 of the coding part of *Cucurbita maxima* DNA. The rest of the sample follows a similar pattern.

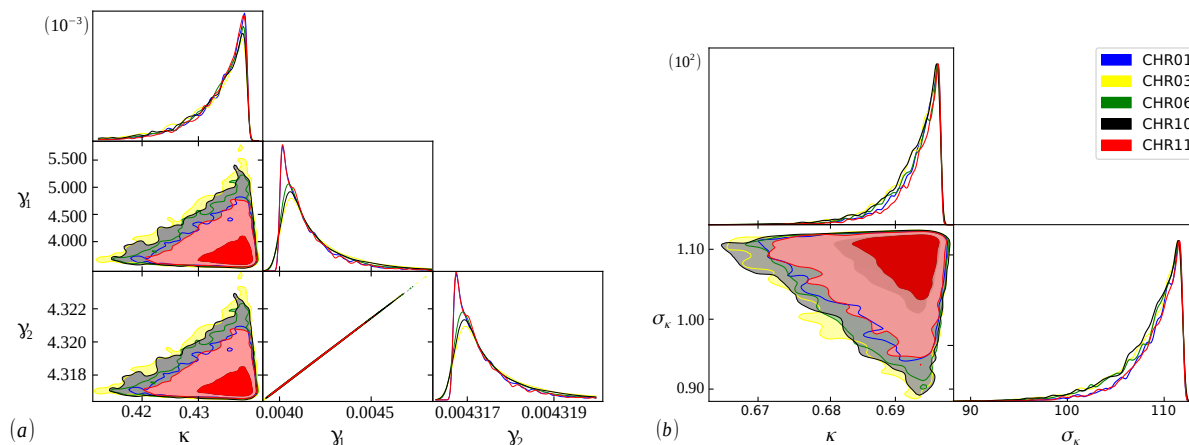


Figure 6. The same as Figure 5, but for chromosomes 01, 03, 06, 10, and 11 of the *Cucurbita moschata* species.

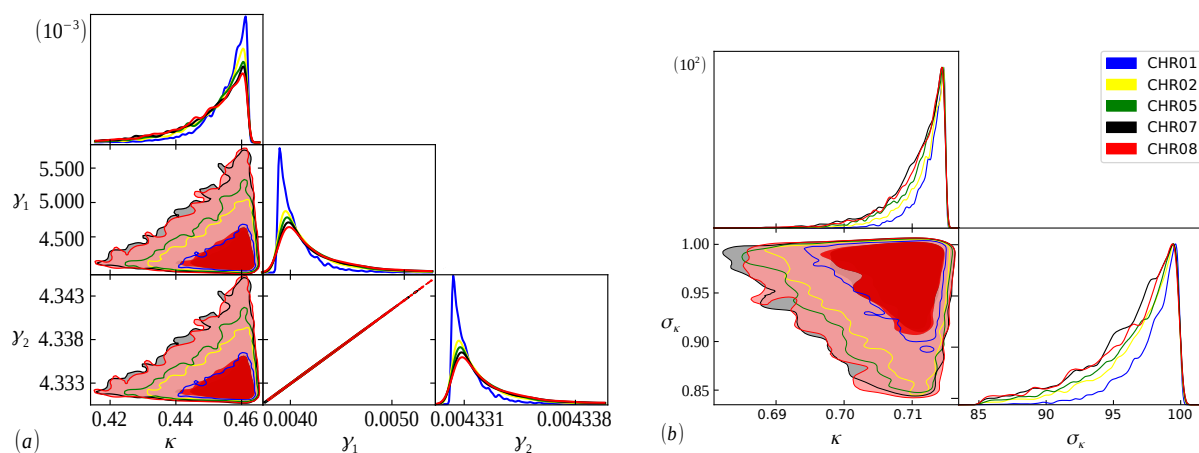


Figure 7. The same as Figure 5, but for chromosomes 01, 02, 05, 07 and 08 of the *Cucurbita pepo* species.

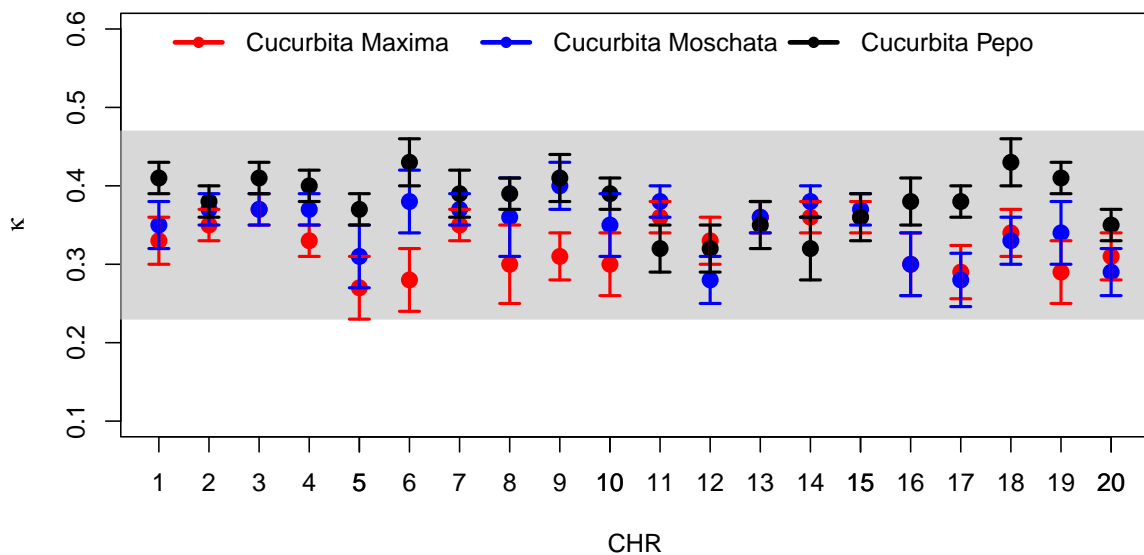


Figure 8. κ values, from the best fit model, Equation (9), for different species. In red, blue, and black, we have, respectively, *Cucurbita maxima*, *Cucurbita moschata*, and *Cucurbita pepo*.

4. Conclusions

A statistical model based on non-additive statistics was developed to describe the size distribution of nucleotide chains in the DNA of species belonging to the *Cucurbitaceae* family, namely *Cucurbita maxima*, *Cucurbita moschata*, and *Cucurbita pepo* [26–28,31]. Specifically, the proposed distribution, Equation (9), expands on a distribution studied in [41] through the sum of the κ -exponentials, which added the parameters γ_1 and γ_2 to capture the statistical correlations between the DNA strands. Another model investigated was the κ -Maxwellian distribution, Equation (11), proposed in [31] for human DNA. We tested the statistical feasibility of models, as well as methods based on Bayesian statistical analysis using the NCBI project database. The cumulative distribution function (9) best fitted the nucleotide base for all chromosomes, of the three species, with the parameter κ belonging to the range (0.27(4); 0.37(2)) for *Cucurbita maxima*, (0.28(3); 0.40(4)) for *Cucurbita moschata*, and (0.32(3); 0.43(3)) in the case of *Cucurbita pepo*. It can be seen in Figure 8 that the values of κ for different species of the coding parts (exons) of the DNA appear to be within a common and relatively narrow range.

Regarding the Bayesian analysis, we compared the κ -exponential-sum distribution with the κ -Maxwellian model. We demonstrated that the first has solid and favorable evidence compared to the κ -Maxwellian distribution. This was reasonably expected given

that the distribution (9) has a free parameter for potential future adjustments. A general task should be to expand the model presented in this study to include additional species, determining whether they fall within the same range of κ for exons (0.35 ± 0.08) discovered for the species investigated here.

Author Contributions: M.M.F.d.L.: Methodology, Writing—Original draft preparation, Software, Visualization, Investigation. D.H.A.L.A.: Conceptualization, Supervision, Formal analysis, Methodology, Writing—Original draft preparation, Writing—Reviewing and editing. R.S.: Visualization, Investigation, Writing—Original draft preparation. G.H.S.N.: Visualization, Investigation, Writing—Original draft preparation. U.L.F.: Visualization, Investigation, Writing—Original draft preparation. M.S.V.: Visualization, Investigation, Writing—Original draft preparation. V.D.M.: Writing—Reviewing and editing. All authors have read and agreed to the published version of the manuscript.

Funding: This study was financed in part by CNPq (Conselho Nacional de Desenvolvimento Científico e tecnológico), and by the Coordenação de Aperfeiçoamento de Pessoal de Nível Superior—Brasil (CAPES). R.S. thanks CNPq (Grant No. 307620/2019-0) for financial support. D.H.A.L.A. thanks CNPq for financial support (CNPq grant No. 317464/2021-3). M.S.V. thanks CNPq (Grant No. 313207/2021-6).

Data Availability Statement: The DNA code data that support the findings of this study are available in NCBI [42].

Acknowledgments: The authors thank William J. da Silva for technical discussions on the Bayesian analysis.

Conflicts of Interest: The authors declare no conflict of interest. The funders had no role in the design of the study; in the collection, analyses, or interpretation of data; in the writing of the manuscript; or in the decision to publish the results.

Appendix A

Table A1. Statistical characteristics of the data after outliers are removed. The first column indicates the chromosome, the second the number of exons, the third and fourth the minimum and maximum lengths. Finally, the quartiles Q1, Q2, and Q3 are in the fifth, sixth, and seventh columns, respectively. In the later columns, we have indicated the same parameters for the other species of *cucurbitaceae*.

CHR	<i>Cucurbita maxima</i>						<i>Cucurbita moschata</i>						<i>Cucurbita pepo</i>					
	N	<i>l_{min}</i>	<i>l_{max}</i>	Q1	Q2	Q3	N	<i>l_{min}</i>	<i>l_{max}</i>	Q1	Q2	Q3	N	<i>l_{min}</i>	<i>l_{max}</i>	Q1	Q2	Q3
1	662	1	2034	166	350	738	667	1	1965	168	357	737	802	3	2049	208	451	833
2	666	1	2229	168	362	710	653	1	2169	165	363	741	663	3	1854	173	380	755
3	641	1	2316	162	352	744	610	1	2207	155	333	740	661	4	1804	172	381	721
4	790	1	2049	198	424	815	851	1	2070	214	458	871	572	4	2004	159	350	687
5	596	1	1967	151	321	650	605	1	1997	154	324	670	623	3	1953	162	352	685
6	654	1	1981	164	343	677	657	1	2147	165	369	747	503	4	1899	146	313	635
7	568	1	2127	143	309	692	608	1	2148	153	343	771	538	3	1917	145	315	650
8	534	2	1857	135	296	587	513	1	1932	130	284	609	578	4	1815	151	339	631
9	610	1	2361	153	320	647	599	1	2363	154	38	753	539	3	1866	152	330	647
10	532	1	2096	134	285	598	616	1	2346	157	342	701	529	4	1995	146	330	703
11	665	1	2001	167	353	753	714	1	2146	179	399	803	588	3	1773	158	337	618
12	557	1	2265	141	302	622	556	1	2133	141	293	610	570	3	1776	150	329	602
13	549	3	2037	141	307	675	605	1	2136	155	338	750	563	3	2092	153	329	606
14	723	1	2181	182	391	786	740	3	2382	188	410	832	534	3	1896	143	311	589
15	601	1	2121	152	325	675	630	1	2190	159	338	673	486	4	1896	137	321	603
16	597	1	2153	150	318	657	601	1	2188	155	333	660	512	3	1872	137	302	649
17	583	2	2052	148	312	614	641	2	1968	164	341	672	507	3	1782	140	333	695
18	574	1	2178	145	320	635	580	1	2016	146	317	624	445	4	2052	129	313	611
19	539	1	2124	137	301	648	555	1	2049	141	310	641	514	3	1884	151	347	697
20	564	1	2212	142	298	628	572	1	2427	145	300	683	501	4	1914	143	316	650

Table A2. Values of κ before and after removing outliers for model (9). (N) represents the number of nucleotides. κ are the best fit values. The subscripts 0 and f represent the values before and after the outliers are removed, (RD) represents the relative difference between them. This behavior is repeated for all chromosomes.

CHR	<i>Cucurbita maxima</i>					<i>Cucurbita moschata</i>					<i>Cucurbita pepo</i>				
	N_0	κ_0	N_f	κ_f	$ RD $	N_0	κ_0	N_f	κ_f	$ RD $	N_0	κ_0	N_f	κ_f	$ RD $
1	687	0.3324	662	0.3336	0.0012	693	0.3455	667	0.3455	0.0000	834	0.4061	802	0.4073	0.0012
2	688	0.3532	666	0.3546	0.0014	675	0.3742	653	0.3749	0.0007	683	0.3812	663	0.3836	0.0024
3	661	0.3749	641	0.3747	0.0002	630	0.3641	610	0.3650	0.0009	682	0.4057	661	0.4076	0.0019
4	828	0.3576	790	0.3330	0.0246	893	0.3677	851	0.3680	0.0003	587	0.4004	572	0.4015	0.0011
5	615	0.2827	596	0.2835	0.0008	623	0.3127	605	0.3123	0.0004	643	0.3661	623	0.3673	0.0012

Table A3. The same as Table A2, but for model (11).

CHR	<i>Cucurbita maxima</i>					<i>Cucurbita moschata</i>					<i>Cucurbita pepo</i>				
	N_0	κ_0	N_f	κ_f	$ RD $	N_0	κ_0	N_f	κ_f	$ RD $	N_0	κ_0	N_f	κ_f	$ RD $
1	687	0.6589	662	0.6590	0.0002	693	0.6648	667	0.6649	0.0001	834	0.6929	802	0.6930	0.0001
2	688	0.6704	666	0.6707	0.0003	675	0.6810	653	0.6811	0.0001	683	0.6919	663	0.6922	0.0003
3	661	0.6760	641	0.6762	0.0000	630	0.6733	610	0.6734	0.0001	682	0.6909	661	0.6911	0.0002
4	828	0.6588	790	0.6592	0.0096	893	0.6633	851	0.6633	0.0000	587	0.7067	572	0.7071	0.0004
5	615	0.6455	596	0.6459	0.0002	623	0.6555	605	0.6556	0.0001	643	0.6881	623	0.6885	0.0004

Table A4. The average of the best fit parameters for the *Cucurbita maxima* species. The sub-index S and M represent the κ -exponential sum function (9) and the κ -Maxwellian function (11), respectively. σ_κ , γ_1 , and γ_2 are free parameters related to the length of the nucleotide chain. The numbers in parenthesis denote the calculated errors.

CHR	N	κ_M	σ_κ	κ_S	γ_1	γ_2
1	662	0.65(1)	97(2)	0.33(3)	0.0067(13)	0.0057(07)
2	666	0.67(1)	101(3)	0.35(2)	0.0054(09)	0.0062(14)
3	641	0.67(1)	95(3)	0.37(2)	0.0069(15)	0.0057(08)
4	790	0.65(1)	94(2)	0.33(2)	0.0067(13)	0.0056(08)
5	596	0.64(1)	102(3)	0.27(4)	0.0054(13)	0.0062(18)
6	654	0.64(1)	96(2)	0.28(4)	0.0056(08)	0.0069(15)
7	568	0.67(1)	92(3)	0.35(2)	0.0059(09)	0.0071(17)
8	534	0.65(1)	94(3)	0.30(5)	0.0060(18)	0.0066(23)
9	610	0.66(1)	103(2)	0.31(3)	0.0051(07)	0.0061(12)
10	532	0.66(1)	99(3)	0.30(4)	0.0053(08)	0.0066(16)
11	665	0.67(1)	96(3)	0.36(2)	0.0069(14)	0.0057(08)
12	557	0.66(1)	90(3)	0.33(3)	0.0059(09)	0.0072(16)
13	549	0.67(1)	95(3)	0.36(2)	0.0067(15)	0.0055(08)
14	723	0.66(1)	96(2)	0.36(2)	0.0068(13)	0.0057(07)
15	601	0.68(1)	91(2)	0.36(2)	0.0068(13)	0.0058(08)
16	597	0.65(1)	98(3)	0.30(4)	0.0067(16)	0.0055(08)
17	583	0.65(1)	102(3)	0.29(4)	0.0051(07)	0.0062(14)
18	574	0.67(1)	93(3)	0.34(3)	0.0070(17)	0.0057(09)
19	539	0.65(1)	98(3)	0.29(4)	0.0065(14)	0.0053(08)
20	564	0.66(1)	101(3)	0.31(3)	0.0052(08)	0.0063(13)

Table A5. The same as Table A4, but for the *Cucurbita moschata* species. The numbers in parenthesis denote the calculated errors.

CHR	<i>N</i>	κ_M	σ_κ	κ_S	γ_1	γ_2
1	667	0.66(1)	95(2)	0.35(3)	0.0069(14)	0.0057(08)
2	653	0.68(1)	97(2)	0.37(3)	0.0054(07)	0.0066(14)
3	610	0.67(1)	96(2)	0.37(3)	0.0068(14)	0.0056(08)
4	851	0.66(1)	96(2)	0.37(3)	0.0071(13)	0.0059(07)
5	605	0.65(1)	103(3)	0.31(2)	0.0052(08)	0.0063(14)
6	657	0.68(1)	97(2)	0.38(4)	0.0065(14)	0.0055(08)
7	608	0.67(1)	92(3)	0.37(3)	0.0074(19)	0.0059(09)
8	513	0.67(1)	88(3)	0.36(2)	0.0074(18)	0.0060(09)
9	599	0.69(1)	96(2)	0.40(4)	0.0054(07)	0.0064(12)
10	616	0.66(1)	98(3)	0.35(3)	0.0068(17)	0.0055(08)
11	714	0.68(1)	99(2)	0.38(2)	0.0054(06)	0.0064(11)
12	556	0.64(1)	99(3)	0.28(3)	0.0054(09)	0.0066(17)
13	605	0.67(1)	104(3)	0.36(3)	0.0051(07)	0.0062(14)
14	740	0.67(1)	95(2)	0.38(3)	0.0059(08)	0.0070(14)
15	630	0.67(1)	90(2)	0.37(4)	0.0070(13)	0.0059(07)
16	601	0.65(1)	107(3)	0.30(3)	0.0049(07)	0.0058(12)
17	641	0.64(1)	105(3)	0.28(3)	0.0061(13)	0.0051(08)
18	580	0.66(1)	99(3)	0.33(4)	0.0064(14)	0.0052(07)
19	555	0.67(1)	99(2)	0.34(3)	0.0051(07)	0.0062(12)
20	572	0.65(1)	110(2)	0.29(2)	0.0047(07)	0.0057(12)

Table A6. The same as Table A4, but for the *Cucurbita pepo* species. The numbers in parenthesis denote the calculated errors.

CHR	<i>N</i>	κ_M	σ_κ	κ_S	γ_1	γ_2
1	802	0.69(1)	88(2)	0.41(2)	0.0072(16)	0.0059(08)
2	663	0.69(1)	97(3)	0.38(2)	0.0053(07)	0.0062(12)
3	661	0.69(1)	84(3)	0.41(2)	0.0064(09)	0.0077(17)
4	572	0.70(1)	95(2)	0.40(2)	0.0062(14)	0.0051(07)
5	623	0.68(1)	96(3)	0.37(2)	0.0061(13)	0.0053(09)
6	503	0.70(1)	75(2)	0.43(3)	0.0070(13)	0.0091(31)
7	538	0.69(1)	87(3)	0.39(3)	0.0059(09)	0.0074(20)
8	578	0.70(1)	94(3)	0.39(2)	0.0061(12)	0.0068(12)
9	539	0.69(1)	77(2)	0.41(3)	0.0088(29)	0.0051(08)
10	529	0.70(1)	94(3)	0.39(2)	0.0063(14)	0.0053(09)
11	588	0.67(1)	109(3)	0.32(3)	0.0045(06)	0.0053(10)
12	570	0.67(1)	96(3)	0.32(3)	0.0063(16)	0.0053(13)
13	563	0.69(1)	92(3)	0.35(3)	0.0053(08)	0.0064(13)
14	534	0.67(1)	95(2)	0.32(4)	0.0053(09)	0.0067(17)
15	486	0.69(1)	88(2)	0.36(3)	0.0066(17)	0.0053(08)
16	512	0.69(1)	90(3)	0.38(3)	0.0055(08)	0.0067(16)
17	507	0.69(1)	94(3)	0.38(2)	0.0065(14)	0.0053(07)
18	445	0.71(1)	77(3)	0.43(3)	0.0074(27)	0.0065(12)
19	514	0.71(1)	93(3)	0.41(2)	0.0065(14)	0.0051(07)
20	501	0.69(1)	106(3)	0.35(2)	0.0045(06)	0.0053(09)

Table A7. Bayesian analysis for exons of each chromosome. The column $\ln(\mathcal{E})$ gives us the Bayesian evidence for each of the models, Equation (11) for (i) and (9) for (j). The indices *max*, *mos*, and *pep* represent, respectively, the species *Cucurbita maxima*, *Cucurbita moschata*, and *Cucurbita pepo*. The numbers in parenthesis indicate the calculated errors.

CHR	κ -Maxwellian			Sum κ -Exponentials			Bayes Factor		
	$\ln(\mathcal{E}_i^{max})$	$\ln(\mathcal{E}_i^{mos})$	$\ln(\mathcal{E}_i^{pep})$	$\ln(\mathcal{E}_j^{max})$	$\ln(\mathcal{E}_j^{mos})$	$\ln(\mathcal{E}_j^{pep})$	$\ln(B_{ij}^{max})$	$\ln(B_{ij}^{mos})$	$\ln(B_{ij}^{pep})$
1	−147.17(1)	−142.12(1)	−170.98(1)	−135.34(1)	−128.84(2)	−152.95(6)	−11.83(1)	−13.28(2)	−18.03(6)
2	−144.46(1)	−137.10(1)	−130.95(1)	−133.29(3)	−125.46(6)	−117.92(1)	−11.17(3)	−11.64(6)	−13.03(1)
3	−138.97(1)	−127.36(1)	−133.76(1)	−128.22(3)	−116.33(1)	−118.96(6)	−10.75(3)	−11.03(1)	−14.80(6)
4	−187.07(1)	−197.18(1)	−107.60(1)	−172.44(7)	−180.54(1)	−97.81(1)	−14.63(7)	−16.64(1)	−9.79 (1)
5	−128.49(1)	−126.69(1)	−121.06(1)	−117.14(3)	−115.10(4)	−108.52(2)	−11.35(3)	−11.59(4)	−12.54(2)
6	−146.70(1)	−137.90(1)	−94.60 (1)	−133.68(2)	−126.53(1)	−83.70(5)	−13.02(2)	−11.37(1)	−10.90(5)
7	−120.97(1)	−131.00(1)	−104.27(1)	−111.31(3)	−119.85(2)	−93.34(3)	−9.66 (3)	−11.15(2)	−10.93(3)
8	−112.37(1)	−103.10(1)	−105.71(1)	−102.26(2)	−93.35(2)	−94.89(2)	−10.11(2)	−9.75 (2)	−10.82(2)
9	−129.29(1)	−120.78(1)	−104.51(1)	−119.07(2)	−111.31(3)	−92.33(1)	−10.22(2)	−9.47 (3)	−12.18(1)
10	−110.92(1)	−132.10(1)	−100.74(1)	−101.87(1)	−120.77(2)	−91.92(3)	−9.05 (1)	−11.33(2)	−8.82 (3)
11	−146.58(1)	−152.99(1)	−108.48(1)	−135.32(1)	−140.62(1)	−97.11(3)	−11.26(1)	−12.37(1)	−11.37(3)
12	−116.96(1)	−114.18(1)	−110.76(1)	−106.53(3)	−102.74(2)	−98.23(6)	−10.43(3)	−11.44(2)	−12.53(6)
13	−114.54(1)	−125.34(1)	−105.07(1)	−105.62(2)	−115.35(3)	−93.44(3)	−8.92 (2)	−9.99 (3)	−11.63(3)
14	−163.94(1)	−163.55(1)	−103.71(1)	−151.50(4)	−150.13(3)	−92.43(1)	−12.44(4)	−13.42(3)	−11.28(1)
15	−126.73(1)	−129.25(1)	−90.10 (1)	−116.28(1)	−116.91(2)	−80.08(2)	−10.45(1)	−12.34(2)	−10.02(2)
16	−130.03(1)	−124.87(1)	−96.78 (1)	−119.19(3)	−114.18(1)	−87.58(1)	−10.84(3)	−10.69(1)	−9.20 (1)
17	−121.57(1)	−135.30(1)	−98.24 (1)	−111.25(2)	−122.31(5)	−89.39(1)	−10.32(2)	−12.99(5)	−8.85 (1)
18	−121.37(1)	−117.42(1)	−84.51 (1)	−111.18(2)	−106.33(1)	−76.01(2)	−10.19(2)	−11.09(1)	−8.50 (2)
19	−114.09(1)	−110.97(1)	−95.81 (1)	−104.59(1)	−101.15(1)	−87.73(1)	−9.50 (1)	−9.82 (1)	−8.08 (1)
20	−117.37(1)	−116.36(1)	−91.77 (1)	−108.02(1)	−106.56(2)	−83.96(1)	−9.35 (1)	−9.80 (2)	−7.81 (1)

References

- Schaefer, H.; Renner, S.S. Phylogenetic relationships in the order Cucurbitales and a new classification of the gourd family (Cucurbitaceae). *Taxon* **2011**, *60*, 122–138. [[CrossRef](#)]
- Eguiarte, L.; Hernández-Rosales, H.; Barrera-Redondo, J.; Castellanos-Morales, G.; Paredes-Torres, L.M.; Sánchez-de la Vega, G.; Ruiz-Mondragón, K.Y.; Vázquez-Lobo, A.; Montes-Hernández, S.; Aguirre-Planter, E.; et al. Domesticación, diversidad y recursos genéticos y genómicos de México: El caso de las calabazas. *TIP Rev. Espec. Cienc. Químico-Biológicas* **2018**, *21*, 85. [[CrossRef](#)]
- Chomicki, G.; Schaefer, H.; Renner, S.S. Origin and domestication of Cucurbitaceae crops: insights from phylogenies, genomics and archaeology. *New Phytol.* **2020**, *226*, 1240–1255. [[CrossRef](#)] [[PubMed](#)]
- Prohens, J.; Nuez, F.; Carena, M.J. *Handbook of Plant Breeding*; Springer: Berlin/Heidelberg, Germany, 2008; pp. 317–349. [[CrossRef](#)]
- Paris, H.S. Genetic resources of pumpkins and squash, *Cucurbita* spp. In *Genetics and Genomics of Cucurbitaceae*; Springer: Berlin/Heidelberg, Germany, 2016; pp. 111–154. [[CrossRef](#)]
- Paris, H.S., History of the Cultivar-Groups of *Cucurbita pepo*. In *Horticultural Reviews*; John Wiley & Sons, Ltd.: Hoboken, NJ, USA, 2000; Chapter 2, pp. 71–170. [[CrossRef](#)]
- Lee, H.Y.; Jang, S.; Yu, C.R.; Kang, B.C.; Chin, J.H.; Song, K. Population structure and genetic diversity of *Cucurbita moschata* based on genome-wide high-quality SNPs. *Plants* **2020**, *10*, 56. [[CrossRef](#)] [[PubMed](#)]
- Weiling, F. Genomanalytische Untersuchungen bei Kürbis (*Cucurbita* L.). *Der Züchter* **1959**, *29*, 161–179. [[CrossRef](#)]
- Sun, H.; Wu, S.; Zhang, G.; Jiao, C.; Guo, S.; Ren, Y.; Zhang, J.; Zhang, H.; Gong, G.; Jia, Z.; et al. Karyotype stability and unbiased fractionation in the paleo-allotetraploid *Cucurbita* genomes. *Mol. Plant* **2017**, *10*, 1293–1306. [[CrossRef](#)] [[PubMed](#)]
- Montero-Pau, J.; Blanca, J.; Bombarely, A.; Ziarsolo, P.; Esteras, C.; Martí-Gómez, C.; Ferriol, M.; Gómez, P.; Jamilena, M.; Mueller, L.; et al. De novo assembly of the zucchini genome reveals a whole-genome duplication associated with the origin of the Cucurbita genus. *Plant Biotechnol. J.* **2018**, *16*, 1161–1171. [[CrossRef](#)]
- Barrera-Redondo, J.; Ibarra-Laclette, E.; Vázquez-Lobo, A.; Gutiérrez-Guerrero, Y.T.; de la Vega, G.S.; Piñero, D.; Montes-Hernández, S.; Lira-Saade, R.; Eguiarte, L.E. The genome of *Cucurbita argyrosperma* (silver-seed gourd) reveals faster rates of protein-coding gene and long noncoding RNA turnover and neofunctionalization within Cucurbita. *Mol. Plant* **2019**, *12*, 506–520. [[CrossRef](#)]
- Peng, C.K.; Buldyrev, S.V.; Goldberger, A.L.; Havlin, S.; Sciortino, F.; Simons, M.; Stanley, H.E. Long-range correlations in nucleotide sequences. *Nature* **1992**, *356*, 168–170. [[CrossRef](#)]
- Li, W.; Kaneko, K. Long-range correlation and partial $1/\alpha$ spectrum in a noncoding DNA sequence. *Europhys. Lett.* **1992**, *17*, 655. [[CrossRef](#)]
- Li, W. The study of correlation structures of DNA sequences: a critical review. *Comput. Chem.* **1997**, *21*, 257–271. [[CrossRef](#)]

15. Arneodo, A.; Bacry, E.; Graves, P.; Muzy, J.F. Characterizing long-range correlations in DNA sequences from wavelet analysis. *Phys. Rev. Lett.* **1995**, *74*, 3293. [CrossRef] [PubMed]
16. Audit, B.; Thermes, C.; Vaillant, C.; d'Aubenton Carafa, Y.; Muzy, J.F.; Arneodo, A. Long-Range Correlations in Genomic DNA: A Signature of the Nucleosomal Structure. *Phys. Rev. Lett.* **2001**, *86*, 6. [CrossRef]
17. Colliva, A.; Pellegrini, R.; Testori, A.; Caselle, M. Ising-model description of long-range correlations in DNA sequences. *Phys. Rev. E* **2015**, *91*, 052703. [CrossRef]
18. Provata, A.; Almirantis, Y. Statistical dynamics of clustering in the genome structure. *J. Stat. Phys.* **2002**, *106*, 23–56. [CrossRef]
19. Karakatsanis, L.P.; Pavlos, E.G.; Tsoulouhas, G.; Stamokostas, G.L.; Mosbruger, T.; Duke, J.L.; Pavlos, G.P.; Monos, D.S. Spatial constrains and information content of sub-genomic regions of the human genome. *iScience* **2021**, *24*, 102048. [CrossRef]
20. Provata, A.; Almirantis, Y. Fractal Cantor patterns in the sequence structure of DNA. *Fractals* **2000**, *8*, 15–27. [CrossRef]
21. Katsaloulis, P.; Theoharis, T.; Provata, A. Statistical distributions of oligonucleotide combinations: Applications in human chromosomes 21 and 22. *Phys. A* **2002**, *316*, 380–396. [CrossRef]
22. Katsaloulis, P.; Theoharis, T.; Zheng, W.; Hao, B.; Bountis, A.; Almirantis, Y.; Provata, A. Long-range correlations of RNA polymerase II promoter sequences across organisms. *Phys. A* **2006**, *366*, 308–322. [CrossRef]
23. Provata, A.; Oikonomou, T. Power law exponents characterizing human DNA. *Phys. Rev. E* **2007**, *75*, 056102. [CrossRef]
24. Gell-Mann, M.; Tsallis, C. *Nonextensive Entropy: Interdisciplinary Applications*; Oxford University Press: Oxford, UK, 2004.
25. Kaniadakis, G. Maximum entropy principle and power-law tailed distributions. *Eur. Phys. J. B* **2009**, *70*, 3–13. [CrossRef]
26. Kaniadakis, G. Non-linear kinetics underlying generalized statistics. *Phys. A* **2001**, *296*, 405–425. [CrossRef]
27. Kaniadakis, G. Statistical mechanics in the context of special relativity. *Phys. Rev. E* **2002**, *66*, 056125. [CrossRef]
28. Kaniadakis, G. Statistical mechanics in the context of special relativity. II. *Phys. Rev. E* **2005**, *72*, 036108. [CrossRef]
29. Kaniadakis, G.; Baldi, M.M.; Deisboeck, T.S.; Hristopulos, G.G.D.T.; Scarfone, A.M.; Sparavigna, A.; Wada, T.; Lucia, U. The κ -statistics approach to epidemiology. *Sci. Rep.* **2020**, *10*, 19949. [CrossRef]
30. Souza, N.; Anselmo, D.; Silva, R.; Vasconcelos, M.; Mello, V. A κ -statistical analysis of the Y-chromosome. *EPL Europhys. Lett.* **2014**, *108*, 38004. [CrossRef]
31. Costa, M.; Silva, R.; Anselmo, D.; Silva, J. Analysis of human DNA through power-law statistics. *Phys. Rev. E* **2019**, *99*, 022112. [CrossRef]
32. Von Toussaint, U. Bayesian inference in physics. *Rev. Mod. Phys.* **2011**, *83*, 943. [CrossRef]
33. Hines, K.E. A primer on Bayesian inference for biophysical systems. *Biophys. J.* **2015**, *108*, 2103–2113. [CrossRef]
34. de Lima, M.M.F.; Silva, R.; Fulco, U.L.; Mello, V.D.; Anselmo, D.H.A.L. Bayesian analysis of plant DNA size distribution via non-additive statistics. *Eur. Phys. J. Plus* **2022**, *137*, 1–8. [CrossRef]
35. Silva, R.; Silva, J.; Anselmo, D.; Alcaniz, J.; da Silva, W.; Costa, M. An alternative description of power law correlations in DNA sequences. *Phys. A* **2020**, *545*, 123735. [CrossRef]
36. Oikonomou, T.; Provata, A.; Tirnakli, U. Nonextensive statistical approach to non-coding human DNA. *Phys. A* **2008**, *387*, 2653–2659. [CrossRef]
37. Oikonomou, T.; Kaloudis, K.; Bagci, G.B. The q -exponentials do not maximize the Rényi entropy. *Phys. A* **2021**, *578*, 126126. [CrossRef]
38. Clementi, F.; Gallegati, M.; Kaniadakis, G. κ -generalized statistics in personal income distribution. *Eur. Phys. J. B* **2007**, *57*, 187–193. [CrossRef]
39. Kaniadakis, G. Theoretical foundations and mathematical formalism of the power-law tailed statistical distributions. *Entropy* **2013**, *15*, 3983–4010. [CrossRef]
40. da Silva, S.L.E. κ -generalised Gutenberg–Richter law and the self-similarity of earthquakes. *Chaos Solitons Fractals* **2021**, *143*, 110622. [CrossRef]
41. Macedo-Filho, A.; Moreira, D.; Silva, R.; da Silva, L.R. Maximum entropy principle for Kaniadakis statistics and networks. *Phys. Lett. A* **2013**, *377*, 842–846. [CrossRef]
42. National Center for Biotechnology Information (NCBI). 2022. Available online: <https://www.ncbi.nlm.nih.gov> (accessed on 17 June 2021).
43. Comparative Genomics (CoGe). 2022. Available online: <https://genomevolution.org> (accessed on 8 June 2021).
44. R Core Team. *R: A Language and Environment for Statistical Computing*; R Foundation for Statistical Computing: Vienna, Austria, 2020.
45. Aguinis, H.; Gottfredson, R.K.; Joo, H. Best-practice recommendations for defining, identifying, and handling outliers. *Organ. Res. Methods* **2013**, *16*, 270–301. [CrossRef]
46. Correia, J.; Silva, R.; Anselmo, D.; da Silva, J. Bayesian inference of length distributions of human DNA. *Chaos Solitons Fractals* **2022**, *160*, 112244. [CrossRef]
47. Almirantis, Y.; Provata, A. Scaling properties of coding and non-coding DNA sequences. *J. Stat. Phys.* **1999**, *97*, 233–262. [CrossRef]
48. van de Schoot, R.; Depaoli, S.; King, R.; Kramer, B.; Märtens, K.; Tadesse, M.G.; Vannucci, M.; Gelman, A.; Veen, D.; Willemesen, J.; et al. Bayesian statistics and modelling. *Nat. Rev. Methods Prim.* **2021**, *1*, 1–26. [CrossRef]
49. Feroz, F.; Hobson, M.P. Multimodal nested sampling: an efficient and robust alternative to Markov Chain Monte Carlo methods for astronomical data analyses. *Mon. Not. R. Astron. Soc.* **2008**, *384*, 449–463. [CrossRef]

50. Feroz, F.; Hobson, M.; Bridges, M. MultiNest: an efficient and robust Bayesian inference tool for cosmology and particle physics. *Mon. Not. R. Astron. Soc.* **2009**, *398*, 1601–1614. [[CrossRef](#)]
51. Feroz, F.; Hobson, M.P.; Cameron, E.; Pettitt, A.N. Importance nested sampling and the MultiNest algorithm. *Open J. Astrophys.* **2013**. [[CrossRef](#)]
52. Skilling, J. Nested sampling. *AIP Conf. Proc.* **2004**, *735*, 395–405. [[CrossRef](#)]
53. Buchner, J.; Georgakakis, A.; Nandra, K.; Hsu, L.; Rangel, C.; Brightman, M.; Merloni, A.; Salvato, M.; Donley, J.; Kocevski, D. X-ray spectral modelling of the AGN obscuring region in the CDFS: Bayesian model selection and catalogue. *Astron. Astrophys.* **2014**, *564*, A125. [[CrossRef](#)]
54. Trotta, R. Bayes in the sky: Bayesian inference and model selection in cosmology. *Contemp. Phys.* **2008**, *49*, 71–104. [[CrossRef](#)]
55. Jeffreys, H. *The Theory of Probability*; OUP Oxford: Oxford, UK, 1998.
56. da Silva, W.; Silva, R. Cosmological perturbations in the Tsallis holographic dark energy scenarios. *Eur. Phys. J. Plus* **2021**, *136*, 1–19. [[CrossRef](#)]